Report

Horses in medieval Kyrgyz: Zooarchaeological analysis of a complete skeletal remain from Ak-Beshim site

Manabu Uetsuki※

※ Research Institute of Cultural Properties, Teikyo University

Abstract

During the 2024 excavation at the Eastern Christian Church district (AKB-8) of Ak-Beshim site in the Kyrgyz Republic, a nearly complete horse skeleton, estimated to belong to a single individual dating to the 11th–12th century, was excavated. The estimated withers height was approximately 135 cm, and the limb proportions were closer to those of draft horses than the Arab horses. The presence of bit-wear suggests that the horse was used for riding. Its estimated age at death was 7–8 years. Butchery marks indicate that horse meat was exploited, but unlike many previous cases at this site, long bones were not fractured. This is the first discovery of a complete horse skeleton at this site, and no similar findings from this period have been reported elsewhere in Kyrgyz. This specimen would serve as a standard for future research on the characteristics of horses in this region.

要旨

キルギス共和国アク・ベシム遺跡の東方キリスト教会地点（AKB-8）の2024年の発掘調査において、同一個体とみられる11～12世紀のウマの全身骨格が出土した。推定体高は約135㎝で、四肢骨プロポーションはアラブ種よりも輓馬（Trait）に近かった。銜跡の存在からは乗用にされたと推定された。死亡年齢は７～８歳であった。解体痕の特徴からは肉の利用が明らかだが、本遺跡で多く見られる長管骨の破砕はされていなかった。ウマの全身骨格の出土は本遺跡では初めてであり、キルギス国内でも同時期の報告例はない。本例は今後、この地域のウマの属性を検討する上で基準となり得るものである。

Keywords: Horse, withers height, limb bone proportion, pathology, butchery marks

I. Introduction

This paper will present the analytical results of a complete medieval horse skeleton excavated from Ak-Beshim site in the central-northern part of the Kyrgyz Republic in Central Asia. The site is an urban ruin formed in the Chu Valley, which extends north of the Tian Shan Mountains. A unique characteristic of the site is the presence of two adjacent cities. The western city (Shahristan 1) was constructed by the Sogdians around the 5th century. On the eastern city (Shahristan 2), the Tang Dynasty, which had expanded westward, established the military outpost of Suyab Garrison（砕葉城）in the late 7th century.

Since 2011, Tokyo National Research Institute for Cultural Properties has conducted excavations at this site, and since 2016, Teikyo University Institute of Cultural Properties has continued excavations in collaboration with the Kyrgyz National Academy of Sciences (Yamauchi & Amanbaeva eds. 2020).

The primary locations where animal remains were excavated are as follows.

- The main street district of Shahristan 1 (AKB-13)
- The Eastern Christian Church district (AKB-8)
- The central district of Shahristan 2 (AKB-15)

At AKB-13 (the main street district), a large number of animal remains were excavated from the street surfaces and the features of adjacent buildings. These remains date primarily to the 8th–10th centuries, with some

extending into the mid-12th century. At AKB-8 (the church district), animal remains were found in trash pits and cultural layers that accumulated after the church was abandoned and repurposed as a residential area. These remains date primarily to the 11th–13th centuries, a slightly later period. The horse remains reported here also belong to this period.

Detailed analysis of animal remains from the site was conducted first by Arai (2016), who examined the animal remains from the main street district of Shahristan 1 (AKB-13). Subsequently, Uetsuki & Arai (2020) compared the animal remains from the earlier phase of Shahristan 1 (AKB-13) and the later phase of the central district of Shahristan 2 (AKB-15). Furthermore, Uetsuki (in press) compared the early and late phases of both Shahristan 1 and 2, revealing differences in animal utilization across different periods and between the two cities.

Since horses are the main subject of this paper, brief summary of the findings from the above studies regarding horses is presented here. Horse remains were frequently excavated at AKB-13 across all periods, whereas they were consistently scarce at AKB-15. A common pattern observed across all districts is a bimodal mortality distribution, with peaks around 5 and 10 years of age. The estimated withers height was approximately 130 cm on average at all districts, showing a similar trend. A notable characteristic is the absence of bit-wears in the specimens examined.

Most animal remains excavated from this site, including those of sheep and cattle, were found in a disarticulated and fragmented state, suggesting that the majority of these animals were ultimately consumed as food. As a result, no horse specimens had been preserved well enough for individual-level analysis.

In the spring of 2024, for the first time at this site, a nearly complete horse skeleton was excavated from the church site (AKB-8). This specimen is ideal for clarifying aspects that previous investigations could not fully determine, such as withers height, limb bone proportions, and pathological features. Additionally, detailed observations revealed numerous butchery marks, indicating that although the skeleton appears to be from a single individual, it was not properly buried. This specimen provides valuable insight into the characteristics of horses used in Ak-Beshim and medieval Kyrgyz, as well as butchering practices of the period. In view of the importance of the material, it was decided to publish this preliminary report ahead of the final excavation report.

II. Materials and Methods

1. Excavation Context

Horse specimens were discovered in the southern half of the excavation area set outside the eastern wall of the church at AKB-8 (Fig.1-Fig.3). They were located at the lower part of a gently sloping area that descends towards the east wall of Shahristan 1. Although its direct relationship to the horse remains is unclear, a layer of rounded pebbles was excavated beneath the horse. The pebble layer also has an inclination, and the horse remains were primarily excavated from the lower part of this depression. Subsequent investigations revealed a large pit extending westward from beneath the pebble layer. The pebbles may have accumulated in the depression formed after the pit was filled, or they may have fallen in due to the subsidence of the fill.

2. Chronology

The radiocarbon dating results related to the horse remains are as follows (2σ calibrated date ranges):

- Horse mandible, right (No.30)
  993-1046 cal AD (85.14%)
  1084-1094 cal AD (2.84%)
  1104-1123 cal AD (6.73%)
  1142-1146 cal AD (0.75%)
- Proximal phalanx, left (No.26)
  1024-1051 cal AD (28.18%)
  1079-1154 cal AD (67.27%)
- Charcoal from Layer 6 of the north-south cross-section belt in Pit 2 (No.2111)
  996-1002 cal AD (2.37%)
  1020-1049 cal AD (42.01%)
  1081-1153 cal AD (51.08%)
- Horse radius from the bottom of Pit 2 (not related to horse remains reported here)
  901-916 cal AD (5.78%)

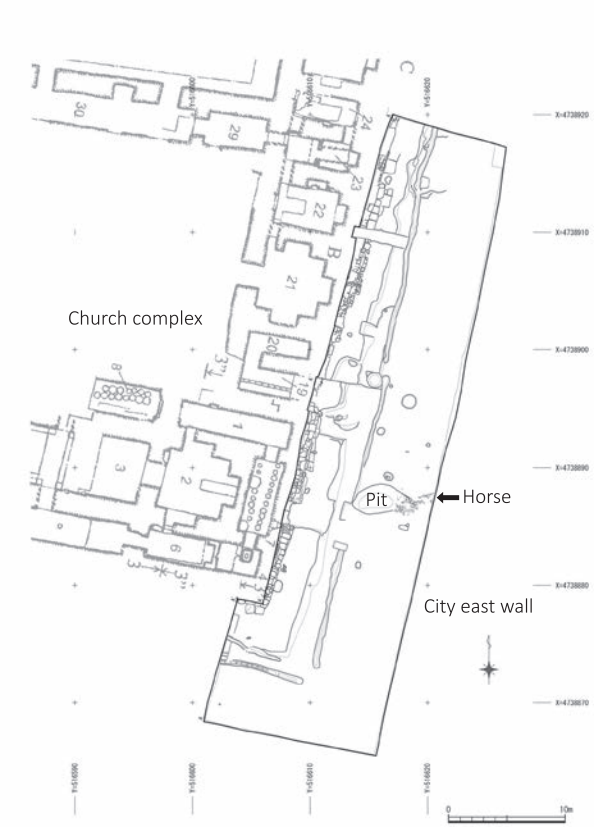

Figure 1 Location of the horse remain

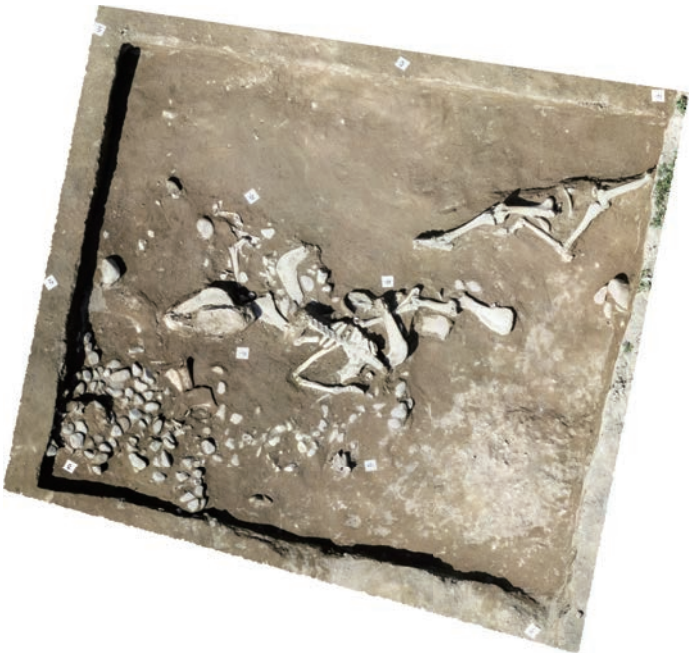

Figure 2 Overhead view of the horse remain

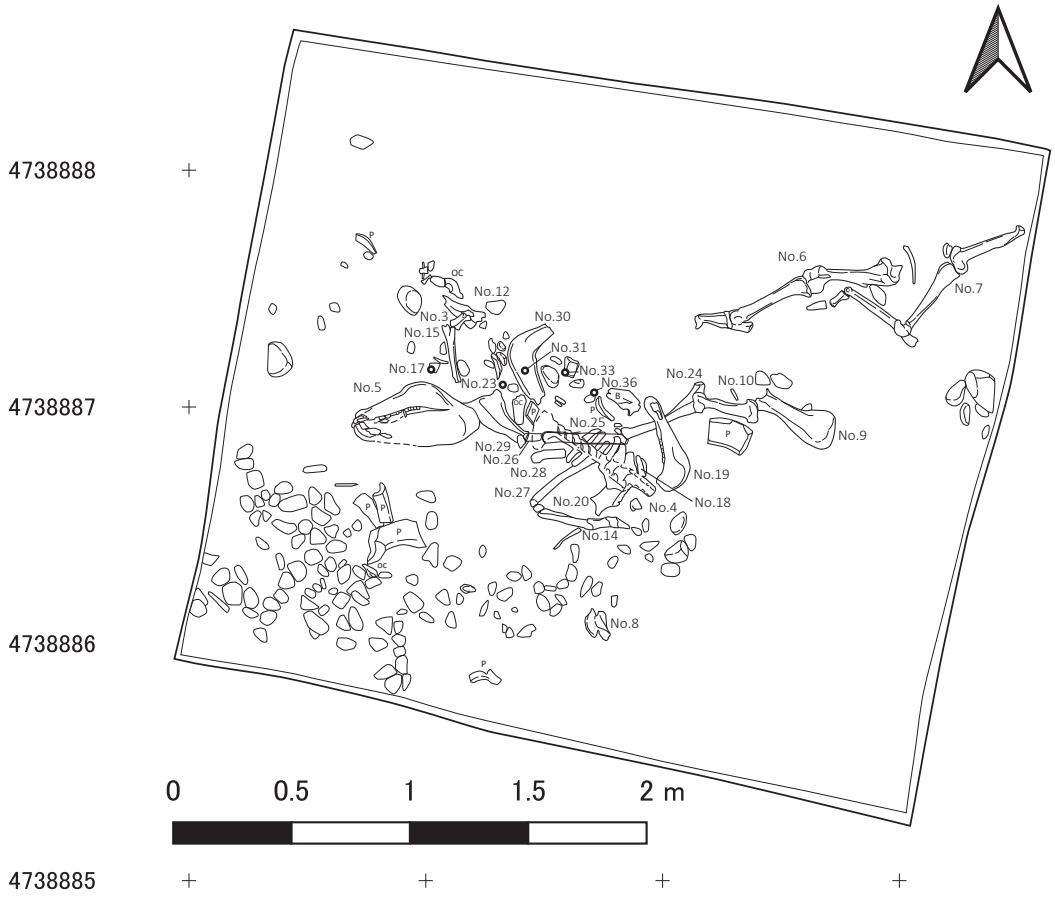

Figure 3 Horse remain (numbers indicate pick up number)

975-1025 cal AD (89.67%)

The bottom of the underlying pit dates to the late 10th to early 11th century, while the upper fill layer dates to the 11th to mid-12th century. The horse remains themselves, specifically mandible B, date to the late 10th to early 12th century. The forelimb (presumably different individual from Skull B) dates from the early 11th to mid-12th century. These dates align with the stratigraphy, and the two horse individuals fall within overlapping timeframes. Therefore, the horse reported here can be dated to the 11th to early 12th century, corresponding to the period when the Kara-Khanid dynasty controlled this region.

3. Methods

Identification was conducted by comparison with modern specimens and reference atlases. Measurements were made following von den Driesch (1976) and Eisenmann (1988). For age estimation based on molars, the formula derived from the central height of the molars, as proposed by Nishinakagawa & Matsumoto (1991) was used. Age assessment results based on the wear patterns of the lower incisors, following Goody (1976), were also taken into consideration. Age estimation based on epiphyseal fusion timing was conducted with reference to Schmid (1972).

For withers height estimation, multiple formulae from Hayashida & Yamauchi (1957), Eisenmann (n.d.), and May (1985) were used. For limb bone proportions, a standardization method based on Eisenmann (1991) was applied, where the total length of each limb bone segment was normalized and compared (“profils centrés réduits”). Specifically, the total length of each part was standardized by subtracting the mean value of the corresponding part from the comparative dataset and dividing it by the standard deviation. The comparative dataset consisted of the same modern breeds as those used in Eisenmann (1991) but updated with additional data from Eisenmann (n.d.). For paleopathological analysis, bit wear on the second premolar of the mandible was recorded following Bendrey (2007a). The ossification of interosseous ligaments in the metapodials was recorded using Bendrey’s criteria (Bendrey 2007b). Other pathological changes and butchery marks were also documented and photographed as necessary.

III. Results

1. Body Part Profiles and Identification of Individuals

Numbers in parenthesis indicate specimen number.

Skull (Sk-A, B, C)

A skull and mandible in articulation were excavated from the westernmost part of the horse bone concentration area (Sk-A, No.5). To the east of this, a mandible from a different individual was found, with the left and right halves slightly apart (Sk-B, No.19 & 30). Although not shown in Fig. 2, further excavation revealed a nearly complete cranium positioned ventral-side up, immediately north of Sk-A (Sk-C, no number). Due to severe deterioration, the skull collapsed upon recovery. As it has not yet been restored, analysis for this specimen has not been conducted. Based on significant molar wear, this specimen was determined to be a different, older individual from Sk-B mandible.

Vertebrae (Ve)

The vertebrae were excavated from the western part of the concentration area, adjacent to the east side of Skull A. The 15th thoracic vertebra to the sacrum, and the first caudal vertebra, was found in articulation, positioned ventral-side up, and excavated from the uppermost part (No.4). Fragments of the left and right ilium (No.18 & 20) were also excavated near the sacrum, suggesting they were originally articulated. Other vertebrae, from the atlas to the thoracic region, were found disarticulated but within the same area.

The vertebral count suggests that these are from a single individual since there are no overlapping, as follows, except for the axis vertebra.

- Atlas: 1 specimen (No.17) It exhibits a bony growth on the dorsal side of the cranial articular surface (Fig. 8).
- Axis: 2 specimens (No.33). No.8 was found slightly apart and is considered a separate individual.
- Cervical vertebrae: 5 specimens (No.12, 36)
- Thoracic vertebrae: 16 specimens (No.4, 23, 31, 36)
- Lumbar vertebrae: 5 specimens (No.4)
- Sacrum: 1 specimen (No.4)
- Caudal vertebra: 1 specimen (No.4)

Forelimbs (FL & FR)

-Left forelimb (FL): Excavated from the central part in the concentration area. The limb remained articulated from the scapula to the distal phalanx. It was in an extended position, with the proximal end oriented eastward.

-Right forelimb (FR): Excavated slightly west in the concentration area. It also remained articulated. Unlike the left limb, it was strongly flexed at the elbow and wrist, forming a "Z-shape," with the proximal end pointing northwest.

Regarding the relationship between the left and right limbs, the measurement values of the ulna and radius were nearly identical, and no morphological differences were observed in any part, suggesting they belong to the same individual.

Hindlimbs (HL & HR)

-Left hindlimb (HL): Excavated from the eastern half in the concentration area. It remained articulated from the femur to the proximal part of the metatarsal bone. It was in an extended position, with the proximal end oriented eastward.

-Right hindlimb (HR): Excavated from the eastern half of the concentration area, in close proximity to the left hindlimb. It remained articulated from the femur to the distal phalanx. It was slightly flexed at the ankle, with the proximal end oriented eastward, similar to the left limb.

Regarding the relationship between the left and right hindlimbs, the measurement values of the tibia, calcaneus, and astragalus were nearly identical, and no morphological differences were observed in any part, suggesting they belong to the same individual.

Relationship Between Forelimbs and Hindlimbs

The relationship between the forelimbs and hindlimbs cannot be definitively determined due to their spatial separation in excavation context. However, based on the estimated withers height discussed later, there is no contradiction in assuming that they belong to the same individual.

Relationship Between Axial Skeleton and Limb Bones

The estimated ages of the two skulls are similar, and the limb bones can only be classified as adult (4.5 years or older) specimens. Therefore, the relationship between the axial skeleton (skull and vertebrae) and the limb bones remains uncertain. There is no significant size difference between the two skulls, making size an unreliable factor for identification of individuals. Based on the excavation context, Skull A is highly likely to have belonged to the same individual as the vertebral column.

Regarding the relationship with the limb bones, it is also highly likely that Skull A, which is nearly complete alongside the vertebrae, belonged to the same individual as the forelimbs and hindlimbs. In contrast, there is little evidence to support that Skull B (mandible only) or Skull C (a cranium excavated from a slightly lower level) belonged to the same individual as the limb bones. In summary, Skull A, the vertebrae, the forelimbs, and the hindlimbs were most likely from the same individual.

2. Skull Observation Results

Sex Determination

For Skull A, canines were not recovered. Since the entire skull was excavated with careful detection work, it is unlikely that they were lost during excavation. All incisors were intact, making it improbable that only the canines decomposed and disappeared. Therefore, Skull A is presumed to be female. Skull B and C is determined to be male since canines were present.

Age Estimation

For Skull A, the estimated age based on the measurable molar heights of both upper and lower, left and right teeth averaged 7.5 years. The wear pattern of the incisors also suggests an age of 7 to 8 years, which aligns with the molar-based estimate. For Skull B, the estimated age based on the measurable molar heights of the lower jaw averaged 8.1 years. The wear pattern of the incisors also suggests an age of around 8 years, thus there is no discrepancy between the estimates. Skull C is estimated to be more than 15 years old from the heavily worn molars.

Measurement Results

Due to damage, only a few measurement values could be directly compared (Tab. 7). Among the comparable mandibula measurements, Skull A was consistently larger. The greatest differences were observed in measurements M3, M6a, M7a, M8a, and M21. However, except for the molar row length, the differences were less than 1 cm and not significant.

Bit Wears (Tab.1, Fig. 7)

Skull A

Exposure of enamel was observed on the mesial side of both the left and right lower P2. The exposed area was relatively large, with a noticeable height difference from the lingual side. The exposed area forms a parallel-sided band. Based on these characteristics, the traces were identified as bit wear. No mesial beveling (Brown & Anthony 1998) on the occlusal surface was observed, but a slight step was noted on the right side. On the upper jaw, the mesial side of left P2 occlusal surface showed partial disappearance of Greaves' effect.

Skull B (mandible)

The exposure of enamel on the mesial side was small on the left side and absent on the right. Since the exposed area on the left was not a parallel-sided band, it could not be classified as bit wear. On the other hand, mesial beveling on the occlusal surface was observed on both sides. On the left side, Greaves' effect was nearly lost.

3. Limb Bone Observation Results

Withers Height Estimation

The results varied significantly depending on the estimation formula, and even when using the same formula, the results differed by elements (Tab. 2, Fig. 4). This variation is due to differences in limb bone proportions, which will be discussed later. In other words, if the limb proportions of the studied specimen differ from those of the species used to derive the estimation formula, the resulting values may significantly deviate from the actual height.

As shown in Tab. 2, the estimation formula that produced the smallest standard deviation in withers height was derived from the tibia. The average estimated withers height using the tibia was 133.0 cm. However, as discussed later, the horse from AKB-8 exhibits a slightly shorter tibia, which should be taken into consideration. The next most reliable estimation, based on the humerus, yielded an average of 136.0 cm, while the overall

Table 1 Bit wear observation

Individual	No.	Element	LR	Teeth measurements (mm)					Anterior enamel exposure						
				L	B	H			EDH(mm)			EDW (mm)	Material	Form	notes
						buc.	cent.	ling.	ant.	buc.	ling.	med.			
Skull A	5	Upper P2	L	37.2	26.7	41	43	-	-	-	-	-	-	-	Greaves' effect at the proximal end slightly more worn out compared to the distal part
		Lower P2	L	32.8	14.7	35	35	32	12.2	0	3.5	2.8	e	y	Recognized as bit wear both in shape and the EDH difference between the anterior and lingual side. The color of enamel is similar to that of cement, but the difference in luster is obvious.
			R	32.0	14.3	35	35	34	10.9	0	6.7	4.3	e	y	The lower anterior edge of the exposure is indistinctly bordered from cementum. The anterior margin of the occlusal surface is slightly stepped and lowered.
Skull B	19	Lower P2	L	29.2	13.9	28	27	-	6.9	0	2.1	2.9	e	n	Anterior exposure mosaic and not parallel. Anterior bevel height=2.6mm. Greaves' effect disappearing.
	30	Lower P2	R	measurements omitted. Refer to left side.					0	0	0	0	-	-	Bevel height 2.7mm. Greaves' effect remaining.

Table 2 Withers height estimation

	GL (cm)	Estimated withers height (cm)							
		Hayashida & Yamauchi (1957)	Eisenmann (n.d.)				May (1985)	mean	SD
			Arab	Przewalskii	Pony	Draft			
Humerus	28.9	135.1	134.4	139.0	136.4	137.3	133.6	136.0	2.0
Femur	39.1	133.3	134.5	138.0	135.3	141.5	136.9	136.6	3.0
Radius	33.4	136.6	134.3	135.6	137.6	144.6	137.3	137.7	3.6
Tibia	33.9	133.8	130.9	131.6	131.6	136.0	133.9	133.0	1.9
MC III	22.2	135.9	129.1	128.2	138.7	144.0	135.6	135.2	5.9
MT III	26.3	130.7	129.0	127.7	134.0	146.7	137.9	134.3	7.1
mean		134.2	132.0	133.4	135.6	141.7	135.9	135.5	3.4
SD		2.1	2.7	4.9	2.6	4.2	1.8	1.7	

Table 3 Limb bone proportion measurements

	GL(mm)								Standradized							
	Humerus	Femur	Radius	Tibia	MC	MT	1PA	1PP	H	F	R	T	MC	MT	1PA	1PP
Trait (5-6)	361.2	469.3	400.0	421.0	263.0	305.7	104.2	104.0	1.52	1.43	1.37	1.43	1.19	1.11	1.38	1.48
Arab (3)	313.7	418.0	361.3	375.7	250.3	296.3	93.3	89.5	0.57	0.57	0.63	0.59	0.84	0.87	0.66	0.56
E. przewalski (23)	265.1	361.4	314.4	328.7	221.0	262.8	79.9	75.5	-0.40	-0.38	-0.26	-0.29	0.03	-0.01	-0.22	-0.33
Tarpan	270.0	375.0	315.0	342.0	203.0	253.0	75.2	71.5	-0.31	-0.16	-0.25	-0.04	-0.47	-0.26	-0.54	-0.59
Pony (12)	212.8	290.8	243.7	258.8	161.0	197.5	60.6	58.6	-1.45	-1.57	-1.61	-1.59	-1.63	-1.71	-1.50	-1.40
AKB8	289.0	391.0	334.0	339.2	222.2	263.3	86.6	85.4	0.07	0.11	0.11	-0.09	0.06	0.01	0.22	0.29
mean	285.3	384.3	328.1	344.2	220.1	263.1	83.3	80.8								
SD	49.9	59.6	52.5	53.8	36.2	38.3	15.1	15.8								

( )=n

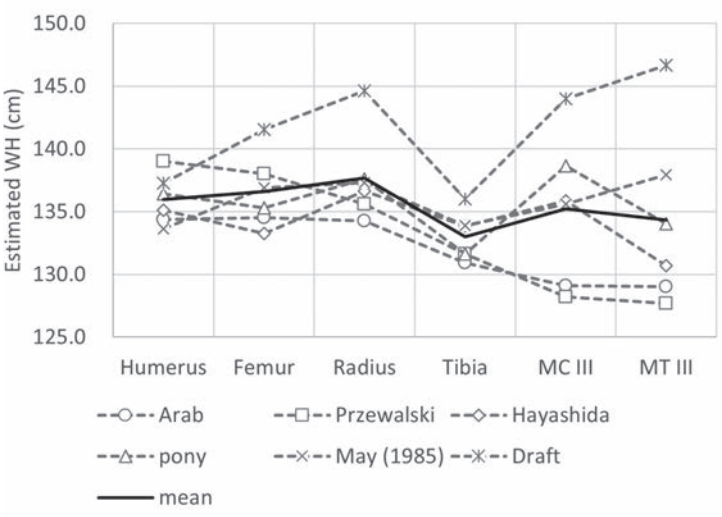

Figure 4 Estimated withers height by various limb bone elements and equations

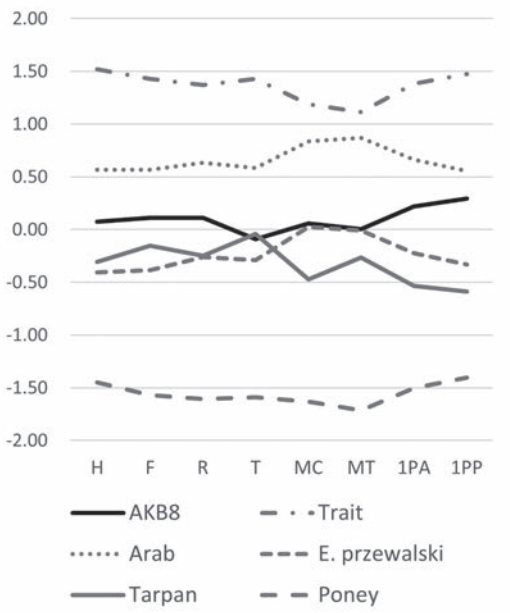

Figure 5 Limb bone proportions (standard: mean of all breeds)

H: humerus F: femur R: radius T: tibia MC: metacarpus MT: metatarsus 1PA: 1st anterior phalange 1PP: 1st posterior phalange

average across all methods was 135.0 cm. Therefore, an estimated withers height of approximately 135 cm is considered reasonable.

Limb Bone Proportions

The standardized results, obtained by subtracting the mean values of the comparative dataset from the total length of the major limb bones and dividing by the standard deviation, are shown in Tab. 3 and Fig. 5. These results follow Eisenmann's (1991) method. The key characteristics of modern horses as documented by Eisenmann can be summarized as follows:

-Arab: Average proportions with slightly elongated metapodials, especially metatarsals.

-Przewalski: Slightly longer femur and radius. Longer metapodials and phalanges (especially in the forelimbs). Mirrors Tarpan.

- Trait (Draft horses): Designed for walking. Long humerus. Slightly short radius. Long phalanges.

- Pony: Resemble draft horses, but the humerus is not particularly long.

- Tarpan: Humerus and femur are approximately equal in length to the tibia. Radius is slightly short. Metapodials and phalanges are short. Mirrors Przewalski.

These can be broadly categorized into the following three groups:

A. Arab and Przewalski is characterized by the longer metapodials.

B. Trait (draft horse) and Pony are similar due to their short metapodials, contrasting with Group A.

C. Tarpan possesses distinct characteristics differing from the other two groups. The most prominent difference is the shorter forelimbs relative to the hindlimbs, which results in noticeable deviations in comparative graphs.

When compared to these groups, the horse from AKB-8 is somewhat similar to Group B due to its shorter metapodials, though the difference is not as pronounced

as in Group B. The notably short tibia observed in the AKB-8 horse is a unique trait not found in any of the other species.

Ossification of Interosseous Ligaments in Metapodials

The degree of ossification in the interosseous ligaments of the metapodials was recorded based on the criteria established by Bendrey (2007b). For the metacarpals, the medial side was classified as "Ib" on both the left and right sides, while the lateral side was classified as "0" (Fig. 11). For the left metatarsal, the medial side was damaged, making its classification indeterminate. On the right metatarsal, both the medial and lateral sides were classified as "0". The right metatarsal of another individual was also classified as "0" for both the medial and lateral sides (Fig. 13). These findings align with Bendrey's (2007b) observations on modern and archaeological horses, which indicate that ossification tends to progress more in the metacarpals than in the metatarsals, and more on the medial side than on the lateral side.

4. Butchery Marks

Numerous fine cut marks were identified in the following locations. Detailed observations of the locations, positions, directions, number, and lengths of the cut marks are presented in Tab.4.

- 1st thoracic vertebra (Fig.8)

Cut marks around the cranial and caudal articular processes and spinous processes were observed.

- Thoracic vertebra (cranial segment, Fig.8)

Longitudinal (cranio-caudal) cut marks were observed on the ventral side of the body.

-Lumbar vertebra (Fig. 9)

On the first, second, and fourth lumbar vertebrae, longitudinal (cranio-caudal) cut marks were observed on the ventral surface of the transverse processes. The third to fifth right-wing areas exhibited old fracture marks, suggesting possible intentional breakage.

- Left scapula (Fig. 10)

Short cut marks were found on the anterior and posterior neck regions. On the inner surface of the blade, long, curved cranio-caudal cut marks were observed.

- Left humerus (Fig. 10)

Transverse (medio-lateral) cut marks were identified on the posterior distal surface.

- Right humerus (Fig. 10)

Table 4 Butchering marks

No.	Group	Element	L/R	Location	Direction	Orientation	Length	Count	Notes
23	Ve	tho	-	cra. art. proc. (left)	dorsal	cra.-caud. (diagonal)	long	many	
23	Ve	tho	-	cra. art. proc. (right)	dorsal	radial	short	many	
23	Ve	tho	-	trans. pro. (right)	lateral ventral	cra.-caud. med.-lat.	long short	3 2	
23	Ve	tho	-	spinous process	right	dors-vent	short	4	
04	Ve	lum(1st)	-	wing (right)	ventral	cra.-caud.	long (med.) & short (lat.)	2	
04	Ve	lum(2nd)	-	wing (left & right)	ventral	cra.-caud.	long (med.) & short (lat.)	3	meander
04	Ve	lum(4th)	-	wing (left)	ventral	cra.-caud.	long	1	
09	FL	sca	L	neck	cranial caudal	med.-lat. cra.-caud.	short short	1 1	
09	FL	sca	L	blade (cra. & caud.)	med	cra.-caud.	long	3	curved
10	FL	hum	L	shaft	cranial	med.-lat.	short	1	
28	FR	hum	R	deltoid tuber.	-	cra.-caud.	short	4	
24	FL	ul	L	olecranon tuber	dorsal	med.-lat.	short	3	
06	HL	fem	L	proximal shaft	cranial	med.-lat.	short	7	
06	HL	fem	L	lesser trochanter	-	cra.-caud.	short	2	
06	HL	fem	L	between head and greater trochanter	-	cra.-caud.	long	5+	
06	HL	fem	L	trochanteric fossa	-	med.-lat.	long	3	
06	HL	fem	L	neck	-	cra.-caud.	long	3	
07	HR	fem	R	lesser trochanter	-	cra.-caud.	short	3	
07	HR	fem	R	distal shaft	medial	cra.-caud.	short	5	
07	HR	fem	R	supra condyle	med. & lat.	med.-lat.	short	2x2	

Multiple short cranio-caudal cut marks were present on the deltoid tuberosity.

- Left ulna (Fig. 11)

Three short transverse (medio-lateral) cut marks were found near the proximal end on dorsal side of olecranon.

- Left femur (Fig. 12)

One to three short cut marks were identified on four different locations along the proximal anterior ridge and lesser trochanter. Multiple cranio-caudal cut marks were observed between the femoral head and the greater trochanter. A long transverse (medio-lateral) cut mark was found carving into the trochanteric fossa. Two cranio-caudal cut marks were identified on the femoral neck below the femoral head.

- Right femur (Fig. 12)

Multiple short cranio-caudal cut marks were found on the lower part (distal) of the lesser trochanter. Several short cranio-caudal cut marks were also identified on the medial side of the femoral shaft and distal portion. On the posterior distal surface, multiple transverse (medio-lateral) cut marks were observed on the medial and lateral supracondylar ridges.

The observed cut marks were primarily found on the thoracic and lumbar vertebrae, as well as the upper limb bones. These are areas with a significant amount of meat attached. Regarding the location of the cut marks on the limb bones, while some were found near the joints, many were also identified on the shaft. These cut marks were likely left not by disarticulation but for filleting meat from the bones. This interpretation aligns with the fact that the limb bones were excavated in an articulated state. Similarly, the long cut marks observed on the ventral surface of the lumbar transverse processes, which were also found in articulation, are likely traces of meat removal.

No distinct cut marks related to skinning were identified, making it unclear whether the hide was utilized. Since no evidence of limb bone breakage was observed, bone marrow was clearly not utilized.

IV. Discussion

1. Comparison with Previously Excavated Horses from Ak-Beshim Site

In this investigation, skulls (one cranium and two mandiles) from one male and one female horse, both around 8 years old, were identified. The relationship between these skulls and the vertebrae and limb bones excavated as a group is unclear. However, if they belong to the same individual, the excavation context suggests that they are most likely associated with the female skull. The following section compares the results of this investigation with previous analyses of horse remains from Ak-Beshim site.

The estimated withers height was approximately 135 cm. In previous investigations, complete specimens with measurable total lengths were rare. As a result, past estimations relied heavily on the total lengths of relatively well-preserved metacarpals and metatarsals, or on limb bone length estimates derived from partial measurements, leading to somewhat reduced accuracy. In both AKB-13 and AKB-15, the average estimated withers height ranged between 132 and 136 cm (Uetsuki & Arai 2020; Uetsuki, in press), which closely aligns with the current findings.

As previously mentioned, withers height estimation based on limb bone length is highly influenced by the limb proportions of the reference breeds and the specific limb bones used in the estimation formula. Regarding limb bone proportions, the present specimen differs significantly from the cursorial Arab horses, as it has relatively short metapodials. Among the breeds compared, it most closely resembles Trait (draft) horse, but differs in having a shorter tibia. Evaluating this unique trait is difficult at present due to the lack of comparable specimens. At the very least, the differences from Arab horses suggest that this individual was not well-adapted for cursoriality.

Evidence of riding use was identified as bit wear in Skull A, observed as mesial wear on the lower P2, and in Skull B, seen as beveling on the occlusal surface. In previous investigations at Ak-Beshim, no horse specimens had been found with such clear evidence of bit wear. This, combined with the exceptionally high proportion of horses among the mammal remains, has been interpreted as evidence that packhorse use for crossing the Tian Shan mountains was predominant at this site (Uetsuki & Arai 2020). The specimen in this

study dates to the post-urban decline period when the site's function, in terms of animal use, is believed to have shifted from a trading city, or consumer to a pastoral settlement, or producer (Uetsuki & Arai 2020; Uetsuki, in press). The identification of clear evidence of riding for the present specimen, which had not been previously observed, is consistent with this proposed transformation of the site's function, as the specimen is from the later phase of the site.

2. Body Part Profile and Butchery Practices

This specimen exhibited butchery characteristics that differed from previous cases. Unlike past findings, no signs of bone cracking were observed in the limb bones, while numerous cut marks were identified. Additionally, both the forelimbs and hindlimbs were found in articulation. This suggests that the butchery process was minimal, and that bone marrow was not utilized. Based on the locations of the cut marks and their placement on the limb bones, it is evident that the meat was harvested for consumption.

In previous investigations, articulated horse bones were extremely rare. Most bones were found in a fragmented state, and the long bone preservation rate of horses was below 20% in both AKB-13 and AKB-15 (Uetsuki & Arai 2020). This pattern was also observed in the remains of other major livestock such as sheep and cattle.

The recovered animal remains were primarily food waste, and the bones were typically broken apart for thorough utilization, including the extraction of marrow. In this regard, the utilization of this specimen appears somewhat atypical. This may be attributed to differences in location and period, as past findings primarily originated from the main street district (AKB-13). However, even at the same AKB-8 district, fragmented specimens are predominant, and no other articulated remains have been found to date. Although at least three skulls were recovered from a limited area this time, the articulated limb bones belonged to only one individual. Given that this case appears to be an isolated example, it is more likely that some incidental factors led to an atypical butchery and utilization process. Therefore, this case cannot be generalized as a standard horse consumption practice during the Kara-Khanid period at this site. However, it does provide insight into one aspect of how horses were butchered and consumed at the time.

V. Conclusion

The horse remains reported here date to the 11th to early 12th century. This period corresponds to the decline of the site's urban functions. At this site, the largest amount of horse remains have been excavated from the main street district of Shahristan 1 (AKB-13). These remains date from approximately the 7th to 12th centuries, though fewer were found in the uppermost layers of the street. Even within Shahristan 1, horses are less frequently found in the church district (AKB-8), where the specimen reported here was excavated. The specimens from AKB-8 mainly dates to the later phase of the site from the 11th century onward (Uetsuki et al. 2023). Similarly, in Shahristan 2, horse remains are consistently rare, regardless of the time period (Uetsuki, in press).

The horse reported in this study was excavated from the later-period church district, and its representativeness of the broader horse population at the site remains uncertain. However, the presence of a nearly complete skeleton has allowed for a multifaceted analysis, including limb bone proportions. Thus, this specimen serves as an important reference for examining the characteristics and utilization of medieval horses, both at this site and in the broader Kyrgyz region.

References

Arai, S. (2016). On the Animal Economy at Medieval Ak Beshim, Kyrgyz Republic. *Bulletin of the Department of Archaeology, the University of Tokyo*, 30: 69-80 (in Japanese with English abstract).

新井才二　2016「キルギス共和国、中世アク・ベシム遺跡の動物経済について」『東京大学考古学研究室研究紀要』

Bendrey, R. (2007a). New methods for the identification of evidence for bitting on horse remains from archaeological sites. *Journal of Archaeological Science*, 34(7), 1036–1050.

Bendrey, R. (2007b). Ossification of the interosseous ligaments between the metapodials in horses: a new recording methodology and preliminary study. *International Journal of Osteoarchaeology*, 17(2), 207–213.

Brown, D., & Anthony, D. (1998). Bit Wear, horseback riding and the Botai site in Kazakhstan. *Journal of Archaeological Science*, 25(4), 331–347.

Eisenmann, V., Alberdi, M.-T., De Giuli, C., Staesche, U. (1988). Volume I: Methodology. In: M. Woodburne, P. Y. Sondaar (eds), *Studying Fossil Horses. Collected papers after the New York International Hipparion Conference*, 1981. Brill, Leiden:1-77.

Eisenmann, V. (1991). Proportions squelettiques de Chevaux quaternaires et actuels. *Geobios*, 24, 25–32.

Eisenmann, V. (n.d.). Withers Height Estimations - [Véra Eisenmann]. Retrieved November 30, 2024, from https://vera-eisenmann.com/withers-height-estimations.

Goody, P. C. (1976). *Horse Anatomy. A Pictorial Approach to the Equine Structure*. J.A. Allen, London.

Hayashida, S., & Yamauchi, T. (1957). Deduction of Withers Height from the Length of the Bone in Horses. *Bulletin of the Faculty of Agriculture, Kagoshima University*, 6: 146-156 (in Japanese with English summary).

林田重幸・山内忠平　1957「馬における骨長より体高の推定法」『鹿児島大学農学部学術報告』

May, E. (1985). Widerristhöhe und Langknochenmaße bei Pferden - ein immer noch aktuelles Problem. *Zeitschrift für Säugetierkunde*, 50, 368–382.

Nishinakagawa, H., & Matsumoto M. (1991). Fundamental research for the identification of excavated bones: a comparative study of bone and tooth measurements in native and modern breeds. *A Study on the Time and Route of the Introduction of Cattle and Horses into Japan, as Examined from Skeletal Remains of Archaeological Sites* (Grant-in-Aid for General Scientific Research (B) Fiscal Year 1990 Report, 164-188 (in Japanese with English summary).

西中川　駿・松元光春　1991「遺跡出土骨同定のための基礎的研究－とくに在来種および現代種の骨、歯の計測値の比較」『古代遺跡出土骨からみたわが国の牛、馬の渡来時期とその経路に関する研究』科学研究費成果報告書.

Schmid, E. (1972). *Atlas of animal bones. For prehistorians, archaeologists and Quaternary geologists*. Amsterdam, New York: Elsevier.

Uetsuki, M. (in press) Ak-Beshim site from the perspective of livestock utilization. *Asia Yūgaku*. Bensei Publishing (in Japanese).

植月学(印刷中)「家畜利用からみたアク・ベシム遺跡」『アジア遊学』 勉誠社

Uetsuki, M. & Arai, S. (2020). Animal Resource Exploitation at Ak-Beshim, Kyrgyz Republic. *Bulletin of Research Institute of Cultural Properties, Teikyo University*, 19, 35-60 (in Japanese).

植月学・新井才二「キルギス共和国アク・ベシム遺跡における動物資源利用」『帝京大学文化財研究所研究報告』19.

Uetsuki, M., Yamauchi, K., & Amanbaeva, B. (2023). Differences in animal resource use and its implications in the two districts of Ak-Beshim site. *JSWAA 28 Abstracts*,47-48. Japanese Society for West Asian Archaeology (in Japanese).

植月学・山内和也・バキット アマンバエバ　2023「アク・ベシム遺跡の二街区における動物資源利用の差とその意味」日本西アジア考古学会編『日本西アジア考古学会第28回総会・大会要旨集』.

Von Den Driesch, A. (1976). *A guide to the measurement of animal bones from archaeological sites*. Peabody Museum Bulletin;1. Cambridge, Mass.: Peabody Museum of Archaeology and Ethnology, Harvard University, 137p.

Yamauchi, K. and Amanbaeva, B. eds. (2020) *Ak-Beshim (Suyab) 2019*. The National Academy of the Sciences of the Kyrgyz Republic, Teikyo University Research Institute of Cultural Properties.

Acknowledgements

I am grateful to Dr. Bakit Amanbaeva (National Academy of the Sciences, Kyrgyz Republic), Professor Kazuya Yamauchi, and Teikyo University Silkroad Scientific Investigation Team for their support and advice during the excavation and analysis. I would also like to thank Askat Jumabaev, Aibek Moldokmatov (National Academy of the Sciences, Kyrgyz Republic), and Rikuo Sakuraba (Teikyo University) for their assistance during the analysis, and Miwa Kawaguchi for preparation of figures. This work was supported by JSPS KAKENHI (21H04984, 23H03924).

Table 5 Molar measurements

Group	Element	No.	L/R	Molar	Age	L	B	Height		
								buc.	cent.	ling.
Skull A	max.	5	L	P2	5.6	37.2	26.7	40.6	43	
			R	M1	7.3	24.7	26.0	47.4	45	
	mand.	5	L	P2	7.7	32.8	14.7	35.1	35	31.6
				P3	8.2	27.0	15.5	45.8	42	42.6
				P4	6.2	27.3	16.1	54.7	54	55.3
				M1	9.1	25.9	14.7	41.9	43	41.7
				M2	7.1	26.0	14.1	54.2	54	52.1
			R	P2	7.7	32.0	14.3	34.5	35	34.3
				P3	8.5	27.5	16.4	43.1	41	41.7
				P4	6.7	27.0	16.9	51.9	51	51.1
				M1	8.8	25.1	15.1	43.9	44	41.3
				M2	7.1	24.8	14.2	56.3	54	53.8
Skull B	mand.	19	L	P2	10.4	29.2	13.9	27.9	27	-
				P3	8.8	26.1	15.1	40.3	40	-
				P4	6.3	25.9	15.3	53.6	53	-
				M1	8.0	23.5	15.4	46	47	-
				M2	8.0	25.7	14.0	49.7	50	-
				M3	-	28.2	11.9	in alveolus		
		30	R	M3	6.8	28.5	12.4	54.5	55	57.1

Table 6 List of identified horse specimens

Group	Element	No.	L/R	Part	Fusion		Count	Wt(g)	Age	Notes
					pro	dis				
Sk-A	crania	05	LR	w	-	-	1	1907.7		Paraloid-B72
	incisor	05	LR	[I123]			1	60.4		Female?
	mandible	05	LR	I123			1	44.2	7~8(incisor), 7.5(molar)	Female? I1: mark, I2: cup bottom, I3: cup=7~8yrs
			L	[P234M123]cor., con.,ang.	-	-	1	429.4		Molar length longer than No.19. Paraloid-B72
			R	[P234M123]cor., con.	-	-	1	430.9		Molar length longer than No.19. Paraloid-B72
Sk-B	mandible	19	LR	L[I123CP234M123] cor., con., ang. R[IxxxCx]			1	494.8	8+-(incisor), 8.1(molar)	Male. I1: mark, I2: cup bottom, I3: wear not complete (but irregular shape). Molar length shorter than No.5.
		30	R	P234M123.body, bra., cor., con., ang.			1	294.7		P2-M2 measurements omitted. Refer to left side.
Ve	atlas	17	-				1	84.5		Lesion (cra. art. dors.)
	axis	33	-	w		+	1	146.8	4.5+-	
	cervical	12	-	w?	c	d	4	232.7	4.5+-	
			-	w?	c	d	-	-	4.5+-	
			-	w?	c	d	-	-	4.5+-	
		36	-	caudal		e	1	10.6		
	thoracic	36	-	w	c	d	1	72.5	4.5+-	1st
		23	-	w	c	+	3	124.8	4.5+-	Cranial portion of tho. Cut marks.
		31	-	w	c	+	5	272	4.5+-	Middle portion of tho.
			-	body	c	f	3	67.2	4.5+-	
		04	-	spine	-	-	1	11		15th?
			-	w	c	+	2	80.1	4.5+-	16-17th. Lesion (17th right cra. art.)
			-	w	c	+	1	47	4.5+-	18th? Lesion (right cra. art.)
		29	-	spine			1	7.6		
	tho/ lum	30	-	spine, art.			3+	30.8		
	lumbar	04	-	w	c	+	1	62.5	4.5+-	1st. Cut marks.
		04	-	w	c	+	4	249.9	4.5+-	2nd-5th. Caudal. Cut marks: 2nd, 4th. Fracture: 3rd-5th right wing.
	sacrum	04	-	w	+	d	1	171.9	4.5+-	Ventral. Fusion line remaining.
	caudal	04	-	w	d	d	1	19		
	rib	31	R	pro			1	2.5		
	pelvis	18	L	fr	-	-	1	49		Ilium
		20	R	fr	-	+	1	90.5		Ilium
FL	scapula	09	L	w	c		1	314.8		Cut marks
	humerua	10	L	w	c	c	1	435.6	3.5<	Cut mark (s. cra)
	radius	24	L	w	c	c	1	272.4	3.5<	
	ulna	24	L	w	c	-	1	68.8	3.5<	Fused with radius. Cut marks. Puncture (head).
	carpal	25	L	w	-	-	1	62.4		car. I., Rad., Ul., Acc., 2, 3, 4
	metacarpus	25	L	w	-	-	1	10.9		2nd
		25	L	w	-	c	1	162.9	1.5<	3rd
		25	L	w	-	-	1	8		4th
	pro. sesamoid	25	L	w	-	-	2	7.4		
	pha1 (ant.)	26	L	w	c	-	1	55.6	1.5<	
	pha2 (ant.)	26	L	axial	c	-	1	13.3	1.5<	
	pha3 (ant.)	26	L	fr	-	-	1	3.2		
FR	scapula	29	R	pro-d.s.	c	x	1	231.4		pro=cranial only
	humerus	28	R	w	c	c	1	395.8	3.5<	Cut marks
	radius	27	R	pro-s, dis	c	c	1	233.2	3.5<	
	ulna	27	R	w	c	-	1	65	3.5<	
	carpal	14	R	w	-	-	1	79.4		car. I., Rad., Ul., Acc., 2, 3, 4
	metacarpus	14	R	w	-	-	1	11.8		2nd
		14	R	w	-	c	1	223.4	1.5<	3rd
		14	R	w	-	-	1	9.5		4th

Table 6 (continued)

Group	Element	No.	L/R	Part	Fusion		Count	Wt(g)	Age	Notes
					pro	dis				
	pha1 ant.	14	R	w	c	-	1	58.7	1.5<	
	pha2 ant.	14	R	w	c	-	1	31.4	1.5<	
	pha3 ant.	14	R	w	-	-	1	15.9		
	pro. sesamoid	14	R	w	-	-	1	7.6		Lateral
	pro. sesamoid	14	R	w	-	-	1	5.6		
	dis. sesamoid	14	R	w	-	-	1	3.2		
HL	femur	06	L	w	c	c	1	645.8	3.5<	Cut marks. Measurement undone.
	tibia	06	L	w	c	c	1	382	3.5<	Lacks distal dorsal and medial
	calcaneus	06	L	w	-	c	1	72.9	3<	
	astragalus	06	L	w	-	-	1	49.7		
	tarsal	06	L	w	-	-	1	32		tar. C, 1+2, 3, 4
	metatarsus	06	L	w	-	-	1	7.2		2nd
		06	L	pro-p.s.	-	-	1	26.5		3rd
		06	L	w	-	-	1	13.9		4th
HR	calcaneus	07	R	w	-	c	1	81.9	3<	
	femur	07	R	w	c	c	1	664.8	3.5<	Cut marks (p.s.-d.s lat., d.s. caud.). Furrow? (head)
	patella	07	R	w	-	-	1	37.7		
	tibia	07	R	w	c	c	1	446.2	3.5<	
	astragalus	07	R	w	-	-	1	68.4		
	tarsal	07	R	w	-	-	1	37.3		tar. C, 3, 4
	metatarsus	07	R	w	-	c	1	245.1	1.5<	3rd
		07	R	w	-	-	1	14.8		4th
	pha1 (post.)	07	R	w	c	-	1	79.6	1.5<	
	pha2 (post.)	07	R	w	c	-	1	37.4	1.5<	
	pha3 (post.)	07	R	w	-	-	1	25.4		Lacks medial
	dis. sesamoid	07	R	w	-	-	1	3		
HR b	metatarsus	15	R	pro-d.s.	-	-	1	6.2		2nd
		15	R	w	-	c	1	278.9	1.5<	3rd
		15	R	pro-s	-	-	1	12.9		4th
	pha1 (post?)	03	R	w	c	-	1	70.2	1.5<	
	pro. sesamoid	15	R	w	-	-	1	7.4		
	pro. sesamoid	15	R	w	-	-	1	7.4		
other individual	axis	08	-	w		f	1	130.3	4.5+-	
	cervical	?	-	w?	c	d	1	65.8	4.5+-	
	ulna	35	L	p.s.	-	-	1	52.7		
	tibia	34	L	pro-s	c	-	1	219.6	3.5<	
	pha3	?	R	w	-	-	1	41.2		

*dis=distal, d.s.=distal shaft, fr=fragment, pro=proximal, p.s.=proximal shaft, s=shaft, w=whole.
Epiphyseal fusion. d=unfused diaphysis,e=unfused epiphysis, f=fusing,+=unfused diaphysis & epiphysis
Descriptions of incisor wear based on Goody (1976). Fragile specimens treated with 5% Paraloid B72 acetone solution are indicated in notes.

Table 7 Bone measurements

Element	L/R	Group	No.	M1		M2		M3		M4		M5		M6		M7		M8		M9		M10		M11		M12		M13		M14		M15		M16		M17	
cra	LR	Sk-A	5	D4	353.0±	D5	123.5	D11	281.6	D14	186.8																								
mand	L	Sk-A	5	D1	x	D2	x	D3	123.3	D4	x	D5	x	D6	x	D6a	168.6	D7	x	D7a	80.3	D8	x	D8a	86.8	D19	219.7	D20	201.8	D21	256.1	D22a	x	D22b	x	D22c	x
mand	R	Sk-A	5	D1	x	D2	x	D3	x	D4	x	D5	x	D6	x	D6a	165.3	D7	82.3	D7a	79.9	D8	x	D8a	85.4	D19	x	D20	x	D21	x	D22a	x	D22b	x	D22c	x
mand	L	Sk-B	19	D1	352+	D2	375+	D3	116.2	D4	241+	D5	273.5	D6	160.4	D6a	154.4	D7	78.6	D7a	76.1	D8	83.3	D8a	80.5	D19	218.7	D20	200.1	D21	250.3	D22a	105	D22b	70.7	D22c	53.8±
at	-	Ve	17	GL	101.8	BFcd	86.5	GLF	95.8																										
axis	-	Ve	33	LCDe	146.8	LAPa	111.3	BFcr	83.1	BPacd	63.0	BPtr	88.2	SBV	44.7	BFcd	46.2	H	101.2																
axis	-	-	8	LCDe	x	LAPa	115.4	BFcr	79.7	BPacd	x	BPtr	x	SBV	46.5	BFcd	x	H	x																
cer	-	Ve	12	GLPa	110.4	BPacd	65.3	BFcr	x	BFcd	x																								
cer	-	Ve	12	GLPa	x	BPacd	66.8	BFcr	x	BFcd	x																								
cer	-	Ve	12	GLPa	105	BPacd	72	BFcr	31.4	BFcd	51.2																								
cer	-	Ve	36	GLPa	x	BPacd	x	BFcr	x	BFcd	59																								
cer	-	Ve	?	GLPa	x	BPacd	x	BFcr	31.3	BFcd	x																								
tho	-	Ve	36	PL	x	BPtr	x	BFcr	30.3	BFcd	58	HFcr	35.3	HFcd	38.8	H	x																		
tho	-	Ve	4	PL	39	BPtr	64.0±	BFcr	42.4	BFcd	45.4	HFcr	40.4	HFcd	41.9	H	113.4																		
lum	-	Ve	4	PL	42	BPtr	213.2	BFcr	42.5	BFcd	47.6	HFcr	35.6	HFcd	40.1	H	116.3																		
sac	-	Ve	4	GL	191.3	PL	175.1	GB	193.5	BFcr	48	HFcr	21.6																						
sca	L	FL	9	1HS	369.5	2DHA	338.1	3Ld	158.5	4SLC	60.5	5GLP	96	6LG	60.3	7BG	50.7																		
sca	R	FR	29	1HS	x	2DHA	x	3Ld	x	4SLC	61.4	5GLP	x	6LG	x	7BG	x																		
hum	L	FL	10	1GL	289	2GLC	273.7	3SD	34.8	4	47.5	5'	71.8	6	103.2	7BT	78.6	8	86.7	9	48.5	10	36.8	11	43.2±	12	37.3	13Bd	83						
hum	R	FR	28	1GL	x	2GLC	x	3SD	x	4	x	5'	x	6	x	7BT	x	8	x	9	x	10	x	11	x	12	x	13Bd	x						
rad	L	FL	24	1GL	334	2Ll	314.6	3SD	38.4	4	27.8	5BFp	77.6	6	39.9	6'	34.3	7Bp	84	8BFd	63.5	9	37.7	10Bd	76.7	11	28.2	12	14.5						
rad	R	FR	27	1GL	x	2Ll	307.2±	3SD	x	4	x	5BFp	79.7	6	42.3	6'	34.7	7Bp	85.4	8BFd	x	9	x	10Bd	x	11	x	12	x						
ul	L	FL	24	1GL	408.5	2LO	84.9	3BPC	42.6	4SDO	44.7	5DPA	63.5																						
ul	R	FR	27	1GL	x	2LO	85.4	3BPC	x	4SDO	44.7	5DPA	63.9																						
car.3	L	FL	25	GB	44.7																														
car.3	R	FR	14	GB	44.5																														
mc3	L	FL	25	1GL	x	2Ll	x	3SD	x	4	x	5Bp	x	6	x	7	x	8	x	9	x	10Bd	x	11	x	12Dd	x	13	x	13'	x	14	x	16	x		
mc3	R	FR	14	1GL	222.2	2Ll	213.5	3SD	33.6	4	26.3	5Bp	49.4	6	30.4	7	39.6	8	15.7	9	6.2	10Bd	47.6	11	50.1	12Dd	36	13	28.8	13'	28.4	14	30.2	16	28.7	
fem	R	HR	7	1GL	391	2GLC	357.7	3SD	38.1	4Bp	117.4	5	83.8	6DC	57.7	7Bd	93.2	8	61.7	9	118.4														
pat	R	HR	7	GL	66.9	GB	65																												
tib	L	HL	6	1GL	x	2Ll	x	2' lat-lat	x	3SD	41.2	4SB	36.1	5Bp	94.5	6Pd	84.5	7Bd	74.2	8Dd	45.9±	9	49.4	10	19	med. L	316.8±								
tib	R	HR	7	1GL	339.2	2Ll	322.9	2' lat-lat	310.5	3SD	39.4	4SB	31	5Bp	94.4	6Pd	82.4	7Bd	74.1	8Dd	44.8	9	47	10	16.8	med. L	316.9								
tal	L	HL	6	1GH	60.8	2LmT	61.4	3	31.5±	3'	42.3	4GB	x	5BFd	55	6	36.5	7	53.6																
tal	R	HR	7	1GH	59.8	2LmT	60	3	30.7	3'	43.9	4GB	62.2	5BFd	53.4	6	36.2	7	52.5																
cal	L	HL	6	1GL	114.9	2	81.5	3	20.6	4	34.9	5	51.7	6GB	53.9	7	51																		
cal	R	HR	7	1GL	114.6	2	81.1	3	20.5	4	34.4	5	51.7	6GB	53.2	7	49.8																		
tar.3	R	HR	7	GB	48.3																														
tar.C	R	HR	7	GB	50.2																														
mt3	R	HR	7	1GL	263.3	2Ll	256.6	3	33	4	31.4	5Bp	50.8	6Dp	38.9	7	45.1	8	11.3	9	7.3	10Bd	47.9	11	51	12Dd	38	13	28.4	13'	28.2	14	3.7			
mt3	R	HR b	15	1GL	254.9	2Ll	247.6	3	33.4	4	29.7	5Bp	49.6	6Dp	40.2	7	44.3	8	12.8	9	8	10Bd	47	11	50.8	12Dd	36.9	13	28.8	13'	27.8	14	31.7			
pha1 ant.	L	FL	26	1GL	86.6	2	77.4±	3SD	34	4Bp	55.2	5Dp	38.1	6Bd	x	7x	59.6±	8	27.5	9	78.4	10x	65.7	11x	x	12x	11.1	13x	x	14BFd	x					
pha1 ant.	R	FR	14	1GL	84	2	76.7	3SD	31.8	4Bp	54.5	5Dp	38.7	6Bd	43.3	7x	52.2	8	25.9	9	74.1	10x	63.6	11x	62	12x	10.6	13x	11	14BFd	43				
pha1 ant.?	R	HR b	3	1GL	80.4	2	74.7	3SD	35.5	4Bp	56.2	5Dp	38	6Bd	45.1	7x	49.9	8	25.7	9	71	10x	58.4	11x	59.1	12x	14.4	13x	15.8	14BFd	42.9				
pha1 post.	R	HR	25	1GL	85.4	2	77.7	3SD	33.8	4Bp	54.5	5Dp	36.9	6Bd	46.4	7x	57.9	8	25.8	9	76.2	10x	66.5	11x	65.1	12x	10.4	13x	10.5	14BFd	44.8				
pha2 ant.	L	FL	26	1GL	49.9±	2	x	3SD	x	4Bp	x	5Dp	x	6Bd	x																				
pha2 ant.	R	FR	14	1GL	48.9	2	38.7	3SD	43.5	4Bp	51.2	5Dp	31.9	6Bd	47.9																				
pha2 post.	R	HR	25	1GL	47.1	2	36.5	3SD	46.3	4Bp	53.3	5Dp	31.9	6Bd	54.1																				
pha3 post.	R	HR	25	1GL	69.8	2Ld	48.4	3GB	x	4BF	x	5	25.1	6HP	44.3±																				
pha3	R	-	?	1GL	58.6	2Ld	54.9	3GB	58.5	4BF	47	5	24.4	6HP	41.1																				
dis. sesa.	R	FR	14	GB	41.2																														

*D+No.=von den Driesch (1976)'s measurement number. (for crania and mandibulae). Numbers for limb bones indicate Eisenmann(1988)'s measurement number. von den Driesch(1976)'s corresponding abbreviations are also added when available.

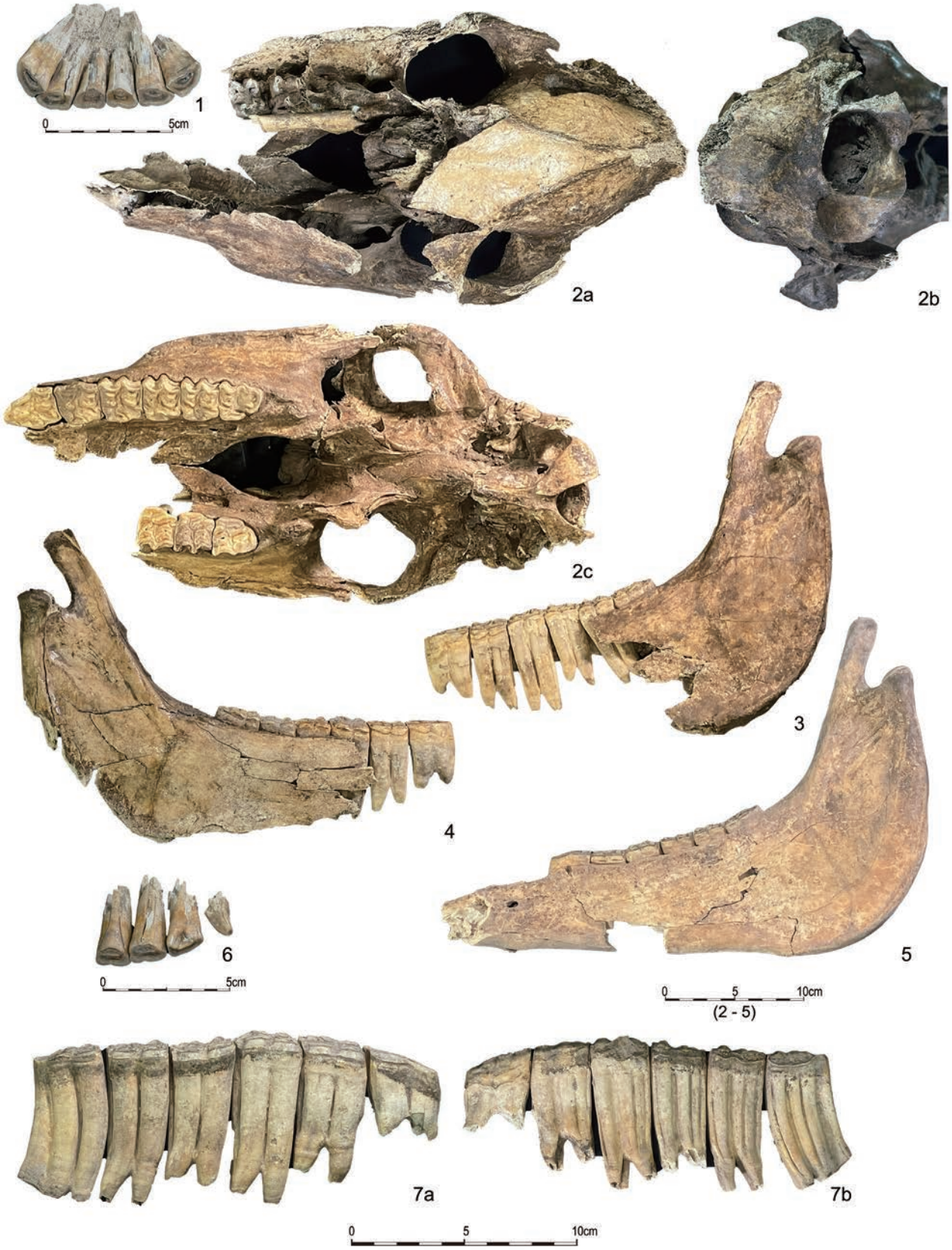

Figure 6 Skull
1. Upper incisors (5) 2. Cranium (5) 3. Mandible L (5) 4. Mandible R (5) 5. Mandible L (19) 6. Lower incisors & canine L (19) 7. Lower molars R, a: buccal, b: lingual (30) Numbers in parenthesis indicate specimen number.

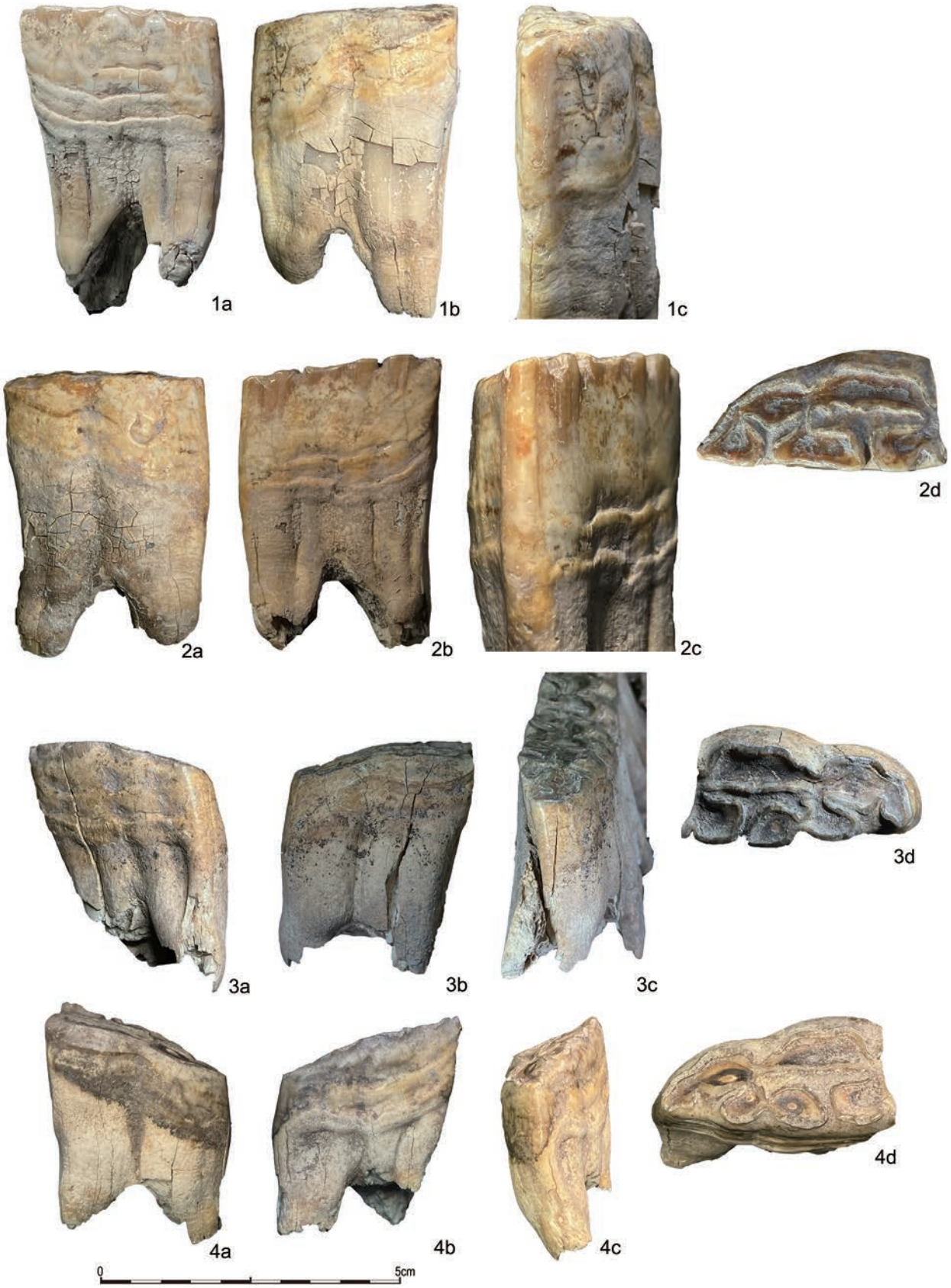

Figure 7 Bit wears
1. P2 L (5) 2. P2 R (5) 3. P2 L (19) 4. P2 R (30) a: buccal, b: lingual, c: anterior, d: occlusal.
The scale represents buccal and lingual only.

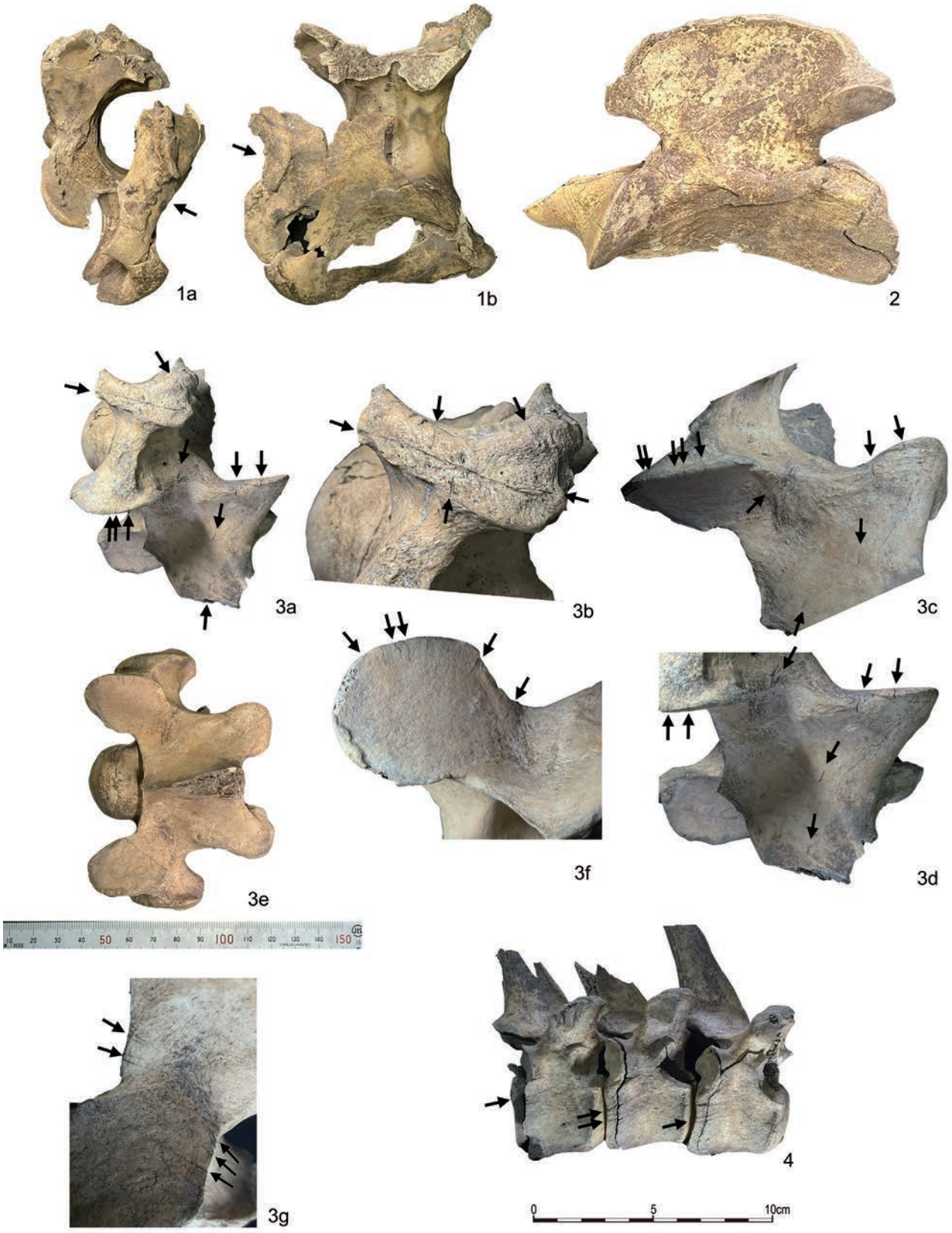

Figure 8 Vertebra (1)
1. Atlas, a: cranial, b: dorsal (17) 2. Axis (33) 3. 1st thoracic, a-d: right side, e: dorsal, f: right cranial articular process, g: left cranial articular process (36). 4. Thoracic, cranial segment (23)
Arrows indicate butchery marks, except for 1, which indicates osteophyte. The scale represents 1, 2, 3e, and 4.

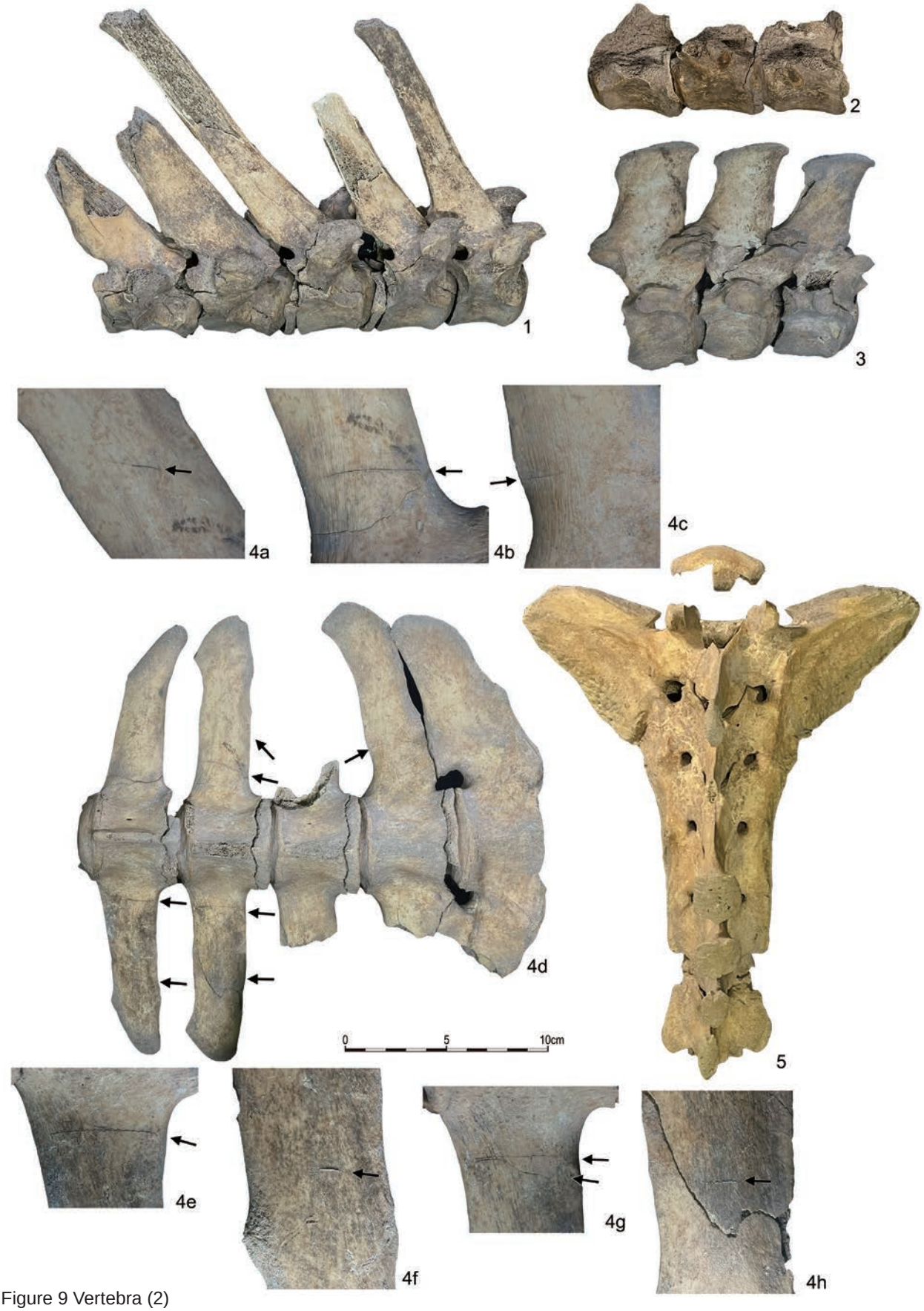

Figure 9 Vertebra (2)
1 & 2. Thoracic, middle segment (31) 3. Thoracic, caudal segment (4) 4. Lumbar, a & b: 2nd left wing, c: 4th left wing, d: ventral, e & f: 1st right wing, g & h: 2nd right wing (4) 5. Sacrum (4). The scale represents 1-3, 4d, and 5.

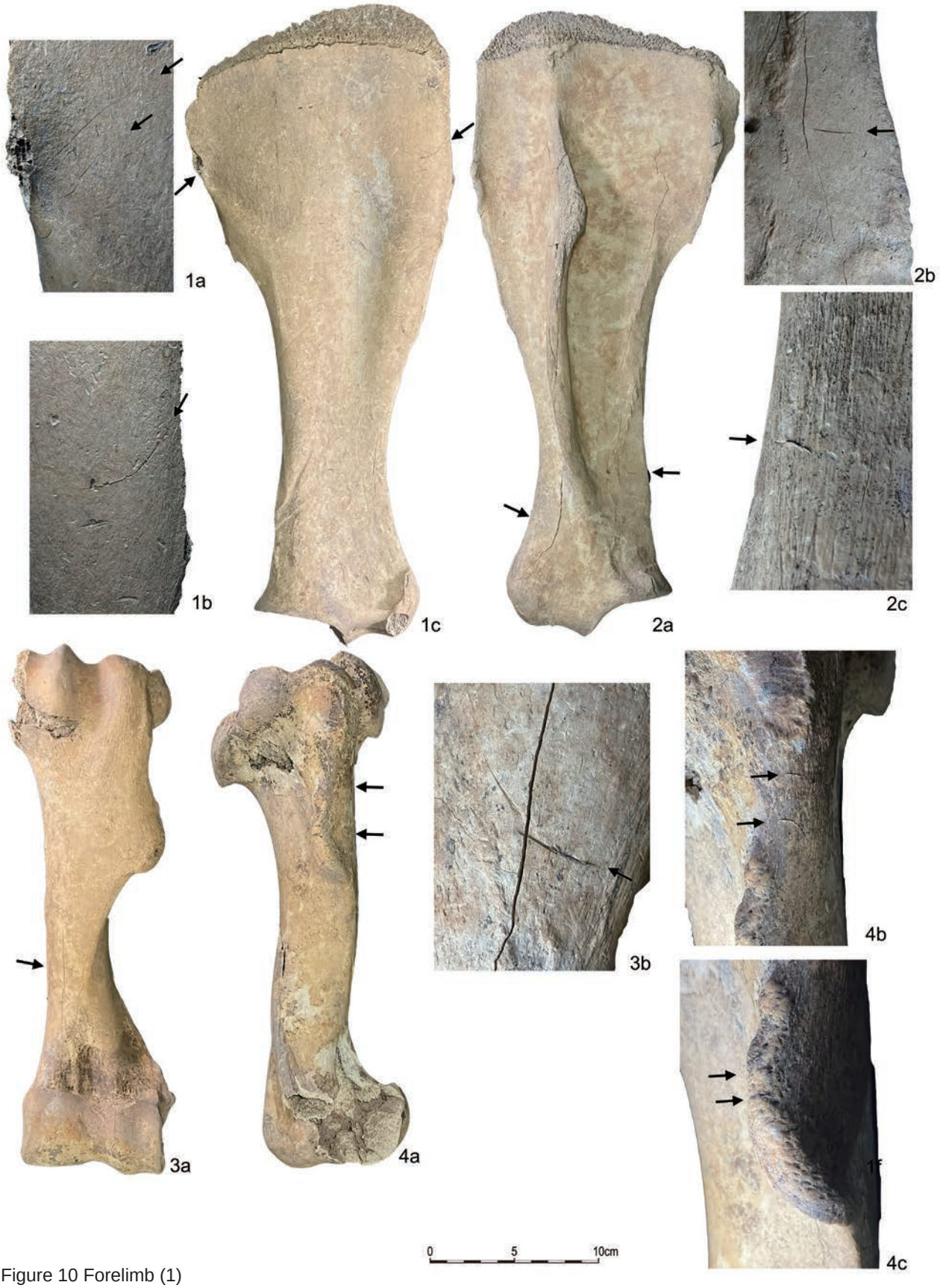

Figure 10 Forelimb (1)
1. Scapula L, a: distocaudal, b: distocranial. c: medial (9) 2. Scapula L, a: lateral, b: neck (caudal), c: neck (cranial) (9) 3. Humerus L, a: cranial, b: humeral crest (10) 4. Humerus R, a: lateral, b & c: deltoid tuberosity (28). Arrows indicate butchery marks. The scale represents 1c, 2a, 3a, and 4a.

Figure 11 Forelimb (2)

1. Radius-ulna L, a: dorsal, b: puncture on medial olecranon, c: butchery marks on dorsal olecranon (24) 2. Metacarpus L, a: dorsal, b: new bone formation on medial edge, c: new bone formation on medial edge of 2nd & 3rd metacarpus (25) 3-6. Phalanges & distal sesamoid R (14) 7-9. 2nd-4th metacarpus R, a: dorsal, b: volar, c: new bone formation on medial edge, d: new bone formation on medial edge of 2nd & 3rd metacarpus (14) 10. Ilium L (18) 11. Ilium R (20) Arrows indicate butchery marks and puncture for 1, and new bone formation for 2b and 8c. The scale represents 1a, 2a, 3-6,8a, 10, and 11.

Figure 12 Hindlimb (1)

1. Femur L, a: cranial, b: lateral ridge, c: proximal shaft, d: lesser trochanter, e: shaft, cranial side of third trochanter, f: caudal, g: proximal, h: trochanteric fossa, i: neck (6) 2. Femur R, a: lesser trochanter, b: distocaudal, c: cranial, d: medial shaft, e: medial distal shaft, f: above lateral condyle, g: above medial condyle, h: medial (7) Arrows indicate butchery marks. The scale represents 1a, 1f, 2c, and 2h.

Figure 13 Hindlimb (2)

1. Patella R, a: cranial, b: caudal (7) 2. Tibia R, a: dorsal, b: plantar (7) 3. 3rd metatarsus R, a: dorsal, b: plantar, c: proximal plantar, no ossification (7) 4-6. 2nd-4th metatarsal R, a: dorsal, b: plantar, c: proximal plantar, no ossification (15) 7. Calcaneus R (7) 8. Astragalus R (7) 9. Central tarsal R (7) 10. 3rd tarsal R (7) 11. 4th tarsal R (7) 12-15. Phalanges & distal sesamoid R (7) The scale represents 1, 2, 3a, 3b, 4, 5a, 5b, 6, 7-15.